7

Angelman Syndrome: Proteomics Analysis of an *UBE3A* Knockout Mouse and Its Implications

Low Hai Loon[1], Chi-Fung Jennifer Chen[2], Chi-Chen Kevin Chen, Tew Wai Loon[1], Hew Choy Sin[3] and Ken-Shiung Chen[1,3,*]

[1] *School of Biological Sciences, Nanyang Technological University,*
[2]*University of Texas, Southwestern Medical School, Dallas, TX,*
[3]*Institute of Advanced Studies, Nanyang Technological University*
[1,3]*Singapore*
[2]*USA*

1. Introduction

Angelman syndrome (AS) is a genetic disorder with an incidence of 1 in 15,000, and it was first described in 1965 by Harry Angelman (1,2). It is characterized by a severe developmental delay together with mental disorders, movement disorders and behavioral abnormalities. Early severe epilepsy, sleep alteration, ataxia, important gait, absence of language and craniofacial dysmorphism are phenotypic characteristics used as diagnostic criteria of AS (3).

Several genetic mechanisms are known to associate with the development of Angelman syndrome including the deletion of 4 Mb region in chromosome 15q11-13, uniparental disomy (UPD), imprinting centre defects, and mutation in *UBE3A* (4). The loss of expression of imprinted genes causes multiple human genetic disorders, including AS and Prader-Willi syndrome (PWS). Although these two diseases are associated with the lack of gene expression from the same chromosome 15q11-q13 region, the clinical features of the two disorders are distinct. Deletion or loss of paternally inherited gene expression results in PWS, while loss of maternally inherited gene expression causes AS (4).

Multiple mouse models have been developed for the study of AS (Table 1). The first reported AS mouse model generated was a mouse with paternal UPD for chromosome 7 (5), followed by another mouse model generated by radiation-induced deletion of *p* locus and *Ube3a* (6). However, these two models carried a large deletion of mouse chromosome 7C that could affect multiple loci (1). In the current study, we used a mouse model which carried an exon 2 deletion of the *Ube3a* gene resulting in a shift in the reading frame, thereby inactivating all putative isoforms of Ube3a (7). If the offspring mice inherited the mutated *Ube3a* allele of maternal origin, the mice will have no Ube3a expression in the cerebellum, Purkinje cells and hippocampus, as *Ube3a* on the paternal chromosome is silenced by genomic imprinting. This mouse model exhibits symptoms similar to that of Angelman syndrome patients, including motor dysfunction, seizures, context-dependant learning deficiency and severely impaired long-term potentiation (LTP) (7).

*Corresponding author

Several proteins that are involved in REDOX (oxidation-reduction reactions) were identified in the 2-D DIGE, including LDH, MDH, GSTs-Mu1, SOD2, and ATP5a1. The result suggested that loss of Ube3a may lead to mitochondrial dysfunction. In addition, the accumulation of Chaperone protein Hsp70 was observed and mRNA levels remained unchanged, suggesting that Hsp70 might be a substrate of Ube3a. Furthermore, NSF, which is known to be involved in neuronal signal transmission, was reduced at protein levels but unaffected at mRNA levels. Finally, CaBP is responsible for binding free calcium ions and may play an inductive role in seizures observed in AS mouse models and patients. TPI1, Triosephosphate isomerase 1, is one of the key enzymes in the glycolysis pathway, while CFL1, Cofilin 1, is known to be a potent regulator of actin filament dynamics. It remains to be determined how differential expression of these proteins may contribute to the development of AS.

	Mutation	Phenotype	Reference
1	*Ube3a* exon 2 deletion	AS	(7)
2	LacZ insertion inactivation of *Ube3a*	AS	(8)
3	insertion/duplication located 13 kb upstream of Snrpn exon 1	AS imprinting mutation	(9)
4	80-kb deletion located upstream of Snrpn exon 1	AS imprinting mutation	(9)
5	*Ube3a-Gabrb3 –Atp10a* deletion	AS	(10)
6	Replacement of mouse PWS-IC with human PWS-IC	PWS and AS imprinting mutation	(11)
7	UPD	AS	(5)
8	GABRB3 inactivation	Some clinical features of AS; 90% of $\beta 3^{-/-}$ mice die within 24 h of birth, survived mice exhibit hyperactive, epileptic seizures, neurological impairments	(12)
9	Transgenic insertion induced deletion; *Zfp127-Herc2* deletion	PWS/AS	(13)

Table 1. Angelman syndrome mouse models

2. Materials and methods

2.1 Protein extraction

Tissue was homogenized in extraction buffer containing 7 M Urea (Cat. No. U5128, Sigma), 2 M Thiourea (Cat. No. RPN 6301, Amersham), 30 mM Tris (Cat. No. 75825, USB), 4% CHAPS (Cat. No. 13361, USB), adjusted to pH 8.5 with HCl. Complete protease inhibitor cocktail (Cat. No. 1697498, Roche) and nuclease mix (Cat. No. 80-6501-42, Amersham) were added into extraction buffer before use. Tissue was homogenized with 3-s pulses followed by 5-s of cooling on ice between the pulses, until no visible tissue

could be observed. The homogenized sample was then transferred to the centrifuge tube and centrifuged at 20,000 x g for 20 min. The supernatant was transferred into a new centrifuge tube and centrifuged for another 20 min at 20,000 x g. The supernatant was then aliquoted and stored at -80ºC. The protein concentration was determined by using Bio-Rad protein assay (Cat. No. 500-0002, Bio-Rad) based on Bradford's method according to the manufacturer's protocol.

2.2 CyDye labelling

Cy2 minimal dye, Cy3 minimal dye, Cy5 minimal dye (Cat. No. 25-8008-60, Cat. No. 25-8008-61, Cat. No. 25-8008-62, Amersham) are the three cyanine dyes used in the experiment. CyDye was reconstituted by using N-N-Dimethylformamide (Cat. No. 22,705-6, Aldrich). 400 pmol of CyDye was used to label 50 µg of protein as recommended by the manufacturer. The labelling reaction was performed on ice for 30 min, quenched with 1 µl of 10 mM lysine (Cat. No. L5501, Sigma) and incubated on ice for 10 min. Cy2 was always used to label the internal control as recommended by the manufacturer. Alternative use of Cy3 and Cy5 for the labelling of wild type and diseased samples prevented labelling bias. In the labelling reaction, the ratio of "dye: protein" was kept low to ensure optimal labelling efficiency.

2.3 1-D isoelectric focusing

Immobiline™ Dry strip, pH 3-11NL, 24 cm strip (Cat. No. 17-6003-77, Amersham) was used for the isoelectric focusing. The strip was rehydrated using rehydration buffer containing 8 M Urea, 4% CHAPS, 1% Pharmalyte 3-11 (Cat. No. 17-6004-40, Amersham), 13 mM DTT (Cat. No. 17-1318-02, Amersham), Destreak solution (Cat. No. 71-5025-39 Amersham). Rehydration was done for 16-18 hr. The rehydrated strip was then transferred to a strip holder and placed on the IPGphor (Cat. No. 80-6414-02, Amersham) that was used for isoelectic focusing. The protein lysate was then applied to the strip by cup loading method, and an equal volume of sample buffer (8 M Urea, 130 mM DTT, 4% CHAPS, 2% Pharmalyte 3-11) was added into the labelled protein sample. The protein was focused on 200 Vhr for each 10 µl of sample applied, followed by 500 Vhr, 1000 Vhr, 1000-8000 V gradient increment for 1hr, and 8000 V for 32,000 Vhr. The strip was equilibrated before it was applied to the 2D electrophoresis unit, first with DTT (Cat. No. 17-1318-02, Amersham) in 10 ml equilibration buffer (6 M Urea, 50 mM Tris-Cl, 30% glycerol, 2% SDS, Bromophenol blue; Glycerol Cat. No. 16374, USB) for 20 min and followed with IAA (Cat. No. RPN 6302, Amersham) for another 20 min.

2.4 2-D gel electrophoresis

The equilibrated strip was transferred to SDS-PAGE and sealed with 1% agarose sealing solution with bromophenol blue (Cat. No. 12370, USB) as trace dye. Gel electrophoresis was performed on 12% acrylamide SDS-PAGE (40% stock, Cat. No. 17-1310-01, Amersham) casted one night before usage, in 2X SDS running buffer (50 mM Tris, 384 mM Glycine, 0.4% SDS; Glycine Cat. No. 161-0718 Bio-Rad, SDS Cat. No. 75819, USB) at 15ºC. 5 W per gel was applied for protein entry, and 10 W per gel for protein separation. The electrophoresis run was stopped when the dye front reached the bottom of the gel. The electrophoresis run was

performed on Ettan DALT *six* system (Cat. No. 80-6485-27, Amersham). The 2-D spot pattern comparison was then made by using Decyder software (Amersham) to figure out protein candidates with significant different steady state levels and those differences in expression were consistent in all 2-D DIGE sample analyzed.

2.5 Silver staining proteins visualization

The acrylamide gel was fixed in 50% Methanol (Cat. No. A-454-4, Fisher), 12% Acetic acid (Cat. No. 1.00063.2511, Merck) overnight with mild shaking. The silver staining was performed using Silver Stain Plus kit (Cat. No. 161-0449, Bio-Rad) according to manufacturer's protocol. The stained gel was then stored in 1% acetic acid solution.

2.6 MALDI-TOF protein identification

Stained gel spots were excised by scalpels and cut into 1 mm^3 cubes. Silver stained gel spots were then destained by using 100 mM Sodium Thiosulfate (Cat. No. A3525, Applichem) and 30 mM Potassium Ferricyanide (III) (Cat. No. 24.402-3, Aldrich) with gentle vortexing. The gel spots were then washed with double distilled water and equilibrated with 100 mM Ammonium Bicarbonate (Cat. No. A6141, Sigma). Gel spots were then dehydrated in Acetonitrile (Cat. No. 34967, Riedel-de Haën). DTT and IAA were added respectively into dehydrated gel spots. The gel spots were then dehydrated again with acetonitrile before 10 ng/µl Trypsin (Cat. No. V5280, Promega) was added for digestion overnight at 37ºC. Peptides were extracted using 50% ACN/5% Trifluoroacetic Acid (TFA). The peptides were then dried using vacuum dry method and cleaned with ZipTip® C_{18} (Cat. No. ZTC 18S 096, Millipore) according to manufacturer's instruction.

2.7 Mouse genomic DNA extraction

Mouse tail was cut and digested in 495 µl NTES buffer (50 mM Tris-Cl, 50 mM EDTA, 100 mM NaCl, 5 mM DTT, 0.5 mM spermidine and 2% SDS) and 5 µl of proteinase K (Cat. No. 13215100, Roche) overnight at 55ºC in a rotary oven. The next day, equilibrated phenol (Cat. No. C2432, Sigma), phenol:chloroform:isomyl alcohol (Cat. No. 75831, USB) and chloroform (Cat. No. 75829, USB) were sequentially used for purification of protein from DNA extract. The genomic DNA was then precipitated by isopropyl alcohol (Cat. No. A415-4, Fisher) and dissolved in TE buffer.

2.8 Mouse genotyping

Three primers named oIMR1965, oIMR1966 and oIMR1967 were used to determine the genotype of the mouse. Primer oIMR1965 was the common primer; when it paired with primer oIMR1966, a 700 bp fragment from the wild type allele would be amplified. On the other hand, when primer oIMR1965 paired with primer oIMR1967, a 320 bp fragment from mutant allele would be amplified. The PCR cycling condition was heat activation at 95ºC for 3 min, followed by 40 cycles of 95ºC for 30 s, 67ºC for 1 min and 72ºC for 1 min; the final extension step was done at 72ºC for 2 min. The PCR product was analyzed by electrophoresis on 1.5% agarose gel.

2.9 Real time RT-PCR

The reaction was performed using iTaq™ SYBR® Green Supermix with ROX (Cat. No. 172-5850, Bio-Rad) containing 2X reaction buffer, 0.4 mM dATP, 0.4 mM dCTP, 0.4 mM dGTP, 0.8 mM dUTP, iTaq DNA polymerase, 6 mM Mg^{+2}, SYBR Green I dye, 1 µM ROX internal reference dye and stabilizers. Reaction volume used was 25 µl, including 12.5 µl of 2X SYBR® Green Supermix, 1 µl of synthesized cDNA, 1 µl of 10 µM forward primer, 1 µl of 10 µM reverse primer [Table 2], topping up with nuclease free water.

Cycling was performed on 7500 Real Time RT-PCR system (Applied Biosystem). Cycling conditions were machine warm up at 50ºC for 2 min, hot initiation at 95ºC for 10 min, cycling condition (45 cycles) of 95ºC for 30 s, 60ºC for 30 s and 72ºC for 2 min, followed by a dissociation stage to generate a melting curve. ΔΔCT method was employed to calculate the differential expression of mRNA in samples examined, by comparing cycling results between target gene and basal control Glyceraldehyde-3-phosphate dehydrogenase (GADPH).

Name	Sequence
HSP70	Sense: 5'-AAG AAC GCG CTC GAG TCC TAT GC-3'
	Anti-sense: 5'-CAC CCT GGT ACA GCC CAC TGA TGA T-3'
CaBP	Sense: 5'-GAT GGC AAC GGA TAC ATA GAT GAA-3'
	Anti-sense: 5'-TCC ATC CGA CAA GGC CAT TAT GTT C-3'
GADPH	Sense: 5'-AGT CTA CTG GTG TCT TCA CCA CCA TGG-3'
	Anti-sense: 5'-TTC TCG TGG TTA ACA CCC ATC AC-3'
VDR	Sense: 5'-AGG TGC AGC GTA AGC GAG AGA T-3'
	Anti-sense: 5'-CCT CAA TGG CAC TTG ACT TAA GC-3'
NeuroD	Sense: 5'-CTC AGT TCT CAG GAC GAG GA-3'
	Anti-sense: 5'-TAG TTC TTG GCC AAG CGC AG-3'
Pax6	Sense: 5'-AGT CAC AGC GGA GTG AAT CAG-3'
	Anti-sense: 5'-AGC CAG GTT GCG AAG AAC-3'
Mash1	Sense: 5'-AGC AGC TGC GGA CGA GCA-3'
	Anti-sense: 5'-CCT GCT TCC AAA GTC CAT TC-3'
LDH	Sense: 5′-AGC AAA GAC TAC TGT GTA ACT GCG A-3′
	Anti-sense: 5′-ACC TCG TAG GCA CTG TCC AC-3′
MDH	Sense: 5′-AGG CTA CCT TGG ACC GGA GCA GTT-3′
	Anti-sense: 5′-GTG GCA GAA CCT GCT CCA GCC TT-3′
Glutathione S-Transferase Mu1	Sense: 5′-TGA CGC TCC CGA CTT TGA CAG AA-3′
	Anti-sense: 5′-TAA GCA AGG AAA TCC ACA TAG GTG-3′
ATP synthase 5a1	Sense: 5′-AGA AGA CTG GCA CAG CTG AGA TGT-3′
	Anti-sense: 5′-CCA GTC TGT CTG TCA CCA AT-3′
SOD2	Sense: 5′-ATG AAA GCC ATC TGC ATC ATT AGC-3′
	Anti-sense: 5′-GCA ATT ATT CCG CAT CCC AAA CG-3′
NSF	Sense: 5'- TGG GGC AGC AGC TTG TCT TTA -3'
	Anti-sense: 5'- TTA GCA CCA AGC CTC CTT TGC -3'

Table 2. Primer sequences used in Real Time RT-PCR analysis:

2.10 Western blot analysis

Protein homogenates were heated in Laemmli sample buffer (Cat. No. 161-0737, Bio-Rad), at 95°C for 10 min. The heated samples were resolved on 12% SDS-PAGE gel and transferred to Immun-Blot PVDF membrane (Cat. No. 162-0177, Bio-Rad) at 100 V for at least 1 hr. The membrane was then blocked with 5% non-fat milk in 0.1% T-TBS (10 mM Tris-Cl, pH 7.5, 150 mM NaCl and 0.1% Tween-20; NaCl Cat. No. 1.06404, Merck, Tween-20 Cat. No. 161-0781, Bio-Rad) for 1 hr at RT. The membrane was then washed three times in 0.1% T-TBS, followed by incubation with primary antibody [Table 3] for 1 hr. The membrane was then washed again three times in 0.1% T-TBS and incubated for 1 hr with HRP conjugated secondary antibody. The membrane was then washed again three times in 0.1% T-TBS before being developed by ECL method (Cat. No. RPN 2108, ECL Western blotting analysis system, Amersham). The blot was stripped with 0.1% T-TBS overnight on an orbital shaker for second antibody detection. The intensity of protein bands detected by Western blot analysis was determined by calibrated densitometer GS-800 and Quantity One 1-D analysis software (Cat. No. 170-7983, Bio-Rad).

Antibody name	Dilution factors used in experiment
Anti-E6AP (Cat. No. A300-352A, Bethyl)	1:2500-5000
Anti Calbindin D-28k (Cat. No. AB1778, Chemicon)	1:2500-5000
Anti-Actin (Cat. No. MAB1501, Chemicon)	1:1000-2500
Secondary HRP conjugated anti-mouse/anti-rabbit (GE Healthcare)	1:2500-5000
Anti-Hsp70 (Cat. No. sc32239 , Santa Cruz)	1:2500-5000
Anti-SOD2 (Cat. No. sc-30080, Santa Cruz)	1:2500-5000
Anti-NSF (Cat. No. ab16681, abcam)	1:10000
Anti-Mash1 (Cat. No. AB155582, Chemicon)	1:2500-5000
Anti-NeuroD (Cat. No. AB155580, Chemicon)	1:2500-5000

Table 3. Antibodies used in experiments

3. Results

In this project, the effects of the loss of UBE3A proteins were investigated using *Ube3a* knockout mice. Two-D DIGE method [Figure 1] was used to identify candidate substrates of Ube3a in the cerebellum and hippocampus; a total of 94 proteins and 74 proteins were initially found differentially expressed in the cerebellum or hippocampus of the *Ube3a* knockout mice, respectively. Next, the protein candidates were tested with the following filtering criteria: 1) proteins appeared in all 2-D DIGE runs examined and 2) the one-way Analysis of Variance (ANOVA) compared protein expression level between the wild type and AS mice indicating the difference is statistically significant. The differentially expressed proteins were then identified by MALDI-TOF with a threshold score of 63. A total of 10 proteins that were successfully identified and fulfilled the filtering criteria are listed in Table 4. An additional 4

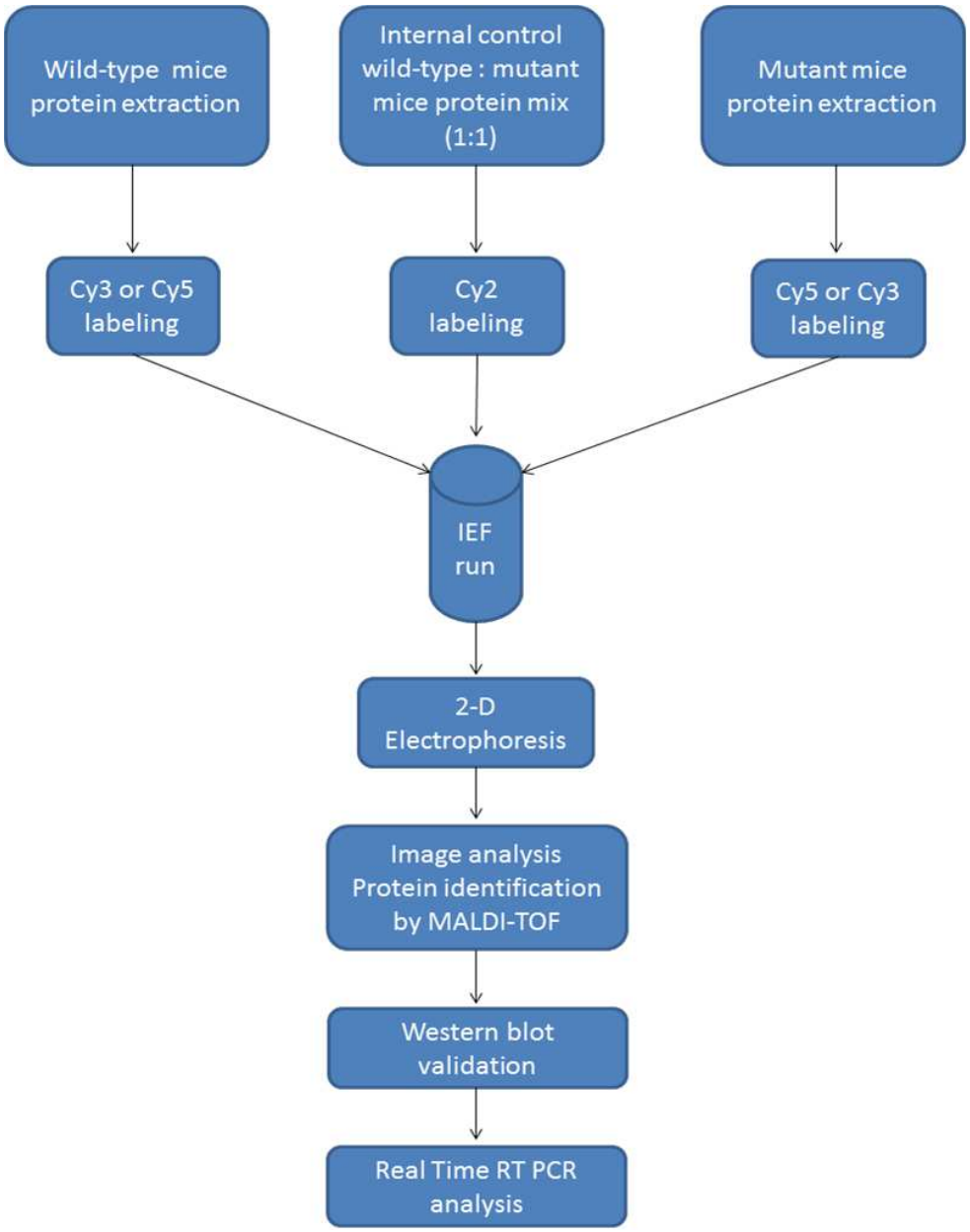

Fig. 1. Work flow of project

proteins, including Mash1, NeuroD, Pax6 and VDR, were not detected in 2-D DIGE runs but were investigated in this project due to the fact that these proteins were shown to be highly associated with one of the proteins identified in this project, CaBP (14). Differentially expressed proteins identified by the 2-D DIGE could be due to the direct, indirect or both direct and indirect effects from the loss of Ube3a expression. Ube3a is known to be involved in proteasome-dependent as well as proteasome-independent functions. Therefore, Western blot analysis was performed to verify the differentially expressed proteins identified by 2-D DIGE analysis and further studied at the mRNA level by Real-Time RT-PCR. It helps to understand that these protein candidates may be affected at the protein level due to impaired protein degradation mechanism (4). Alternatively, these proteins may be affected at the transcriptional level, as Ube3a is also involved in transcriptional regulation (15).

By comparing protein samples from wild type mice and AS mice in the 2-D DIGE study, protein candidates that showed differential expression were found and identified by the MALDI-TOF method. Western blot was then employed to confirm the differential expression observed in 2-D DIGE. Real time RT-PCR was used to detect any differences at the transcriptional level in the protein candidates identified.

Protein identified by MALDI-TOF	pI	Molecular Weight	Accession number	Sequence coverage %	Score	Function
CABP	4.82	25943	P12658	50%	375	Calcium ion buffer
HSP70	5.52	70079	NP_034609.2	24%	358	Protein folding and degradation
SOD2	8.80	24602	P09671	30%	219	REDOX
LDH	7.61	36498	P06151	7%	134	REDOX
MDH	6.16	36477	gi|92087001	30%	365	REDOX
GSTs-Mu1	7.72	25969	P10649	35%	319	REDOX
NSF	6.52	82613	gi|29789104	29%	162	Docking and fusion of synaptic vesicles
ATP5a1	9.22	59752	gi|6680748	49%	436	ATP synthesis
Cofilin 1, non muscle	8.22	18776	gi|6680924	22%	116	Disassembles actin filaments
TPI1 (Triosephosphate isomerase 1)	6.90	27038	gi|6678413	56%	489	Glycolysis, energy production

Table 4. Differentially expressed proteins detected by 2-D DIGE

3.1 2-D DIGE and silver staining

After the Decyder software analysis was performed by using analytical gel (CyDye labelled), another set of protein electrophoresis (preparative gel) were performed using 600 µg of unlabelled protein sample. The protein samples used in the preparative gel were the same as those used for 2-D DIGE analysis. After electrophoresis, silver staining was conducted to visualize protein spots on the gel. Typically, 800-1000 protein spots were visualized on each gel [Figure 2].

Fig. 2. Silver staining of acrylamide gel after SDS-electrophoresis
Protein extract (600 µg) from cerebellum was loaded in a first dimension IPG strip (pH3-11, NL, 24 cm; Running time: 15.5 hr, approx 47 kVh) and resolved in 12.5% acrylamide gel (Running time: 5.15 hr, 10 W per gel). Proteins were visualized by silver staining. These gels are called preparative gels, and they contain more protein content to allow for subsequent analyses including silver staining and MALDI-TOF. CyDye labelled proteins were run on analytical gels which are scanned by lasers and thus do not require a high quantity of proteins.

3.2 Detection and identification of differentially expressed protein in AS versus wild type brain tissue

A total of ten differentially expressed proteins were detected by using 2-D DIGE from protein samples extracted from the cerebellum or hippocampus of wild type mice and AS mice (*Ube3a* knockout). The protein spots were recovered from silver-stained acrylamide gels run in parallel, and identification was made based on the protein profile generated by MALDI-TOF [Figure 3] with a threshold score of 63. All candidates were confirmed at least

twice in separate 2-D DIGE runs and MALDI-TOF identification. Another four bHLH proteins, including Mash1, NeuroD, Pax6 and VDR, were also studied in this project, as the proteins are highly related to CaBP (14).

A total of eight proteins studied are involved in REDOX reactions, including HSP70, SOD2, MDH, LDH, VDR, GSTs-Mu1, ATP5a1 and CaBP. Four of the bHLH proteins, VDR, Pax6, Mash1 and NeuroD are involved in neuronal cell differentiation, while NSF is crucial in synaptic vesicle transmission and learning processes that are controlled by the hippocampus [Figure 4]. TPI1 is involved in energy production, while Cofilin 1 is involved in actin disassembly and may also be involved in neuronal signal transduction.

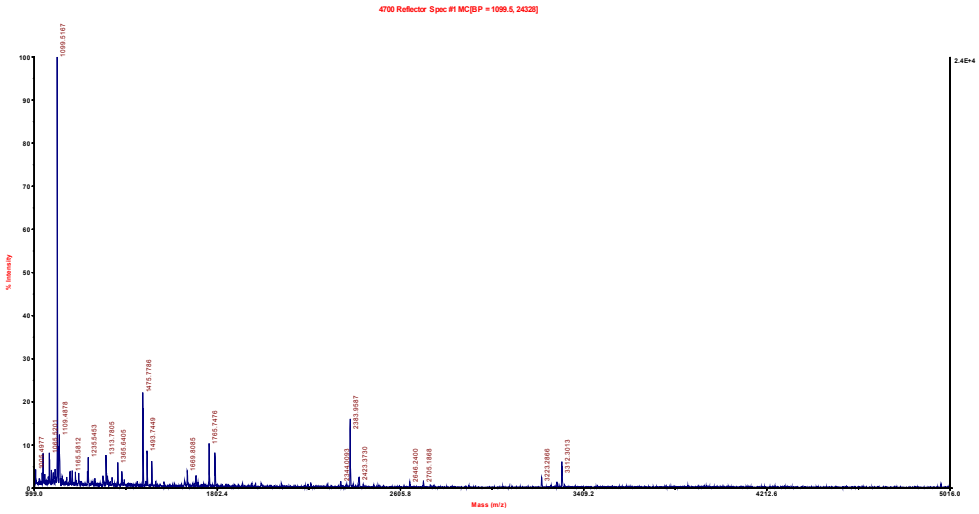

Fig. 3. Protein identification by MALDI-TOF
MS spectrum for one of the proteins identified- CaBP. After peptide detection, the peptide profile was used to match the NCBI database for protein identification.

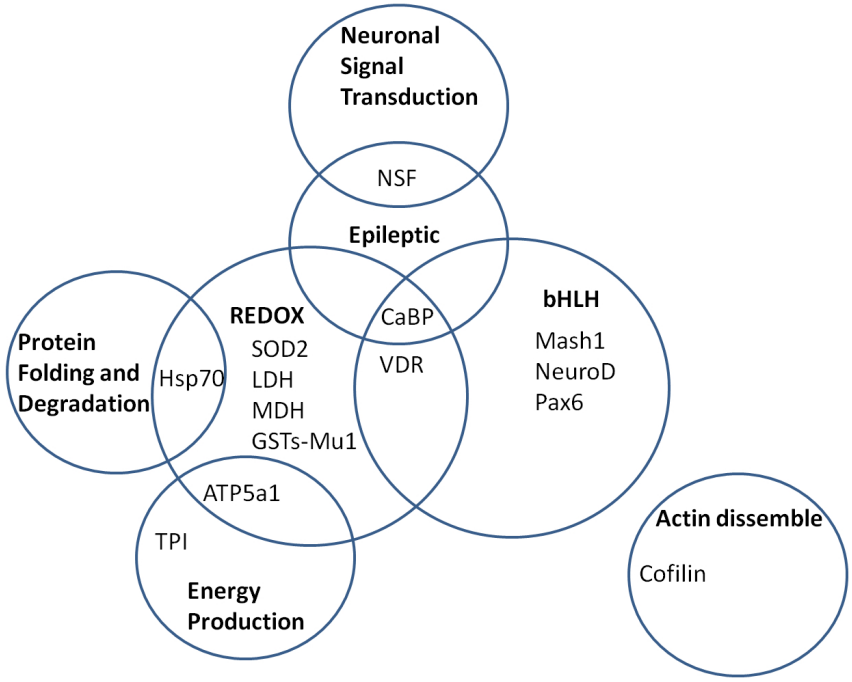

Fig. 4. 2-D DIGE results and inter-connected functions of the identified proteins. This figure shows differentially expressed proteins categorized by their functions. Some proteins are known to be involved in multiple pathways and functions.

3.3 Validation of 2-D DIGE/MS results by Western blot analysis

Western blot was conducted to validate the differentially expressed proteins that were identified in 2-D DIGE/MS. In the cerebellum, three proteins, including SOD2, CaBP and Mash1, were down-regulated in Ube3a knockout mice [Figure 5], while Hsp70, NSF and NeuroD were accumulated in knockout mice [Figure 6]. However, SOD2, Mash1, CaBP, NeuroD and NSF were down-regulated [Figure 7] and HSP70 was accumulated [Figure 8] in the hippocampus of *Ube3a* knockout mice. The Western blots were repeated at least three times by using different sets of cerebellum and hippocampus tissues [Figures 5-8].

In the cerebellum, Hsp70 was found to be up-regulated by approximately 120% based on the densitometer scan results. NSF and NeuroD were up-regulated by 85% and 50%, respectively. SOD2 was down-regulated by 45% in the cerebellum of *Ube3a* knockout mice. Based on densitometer scan results, CaBP and Mash1 were both found to be reduced by approximately 75% in defective mice.

In the hippocampus, Hsp70 was increased by 50% when samples from wild type mice were compared to defective mice. SOD2 and Mash1 were both reduced by approximately 80% in *Ube3a* knockout mice; CaBP and NeuroD were found down-regulated by 40% and 45%, respectively, when compared to the wild type sample. Lastly, NSF was reduced by nearly 50% in *Ube3a* knockout mice.

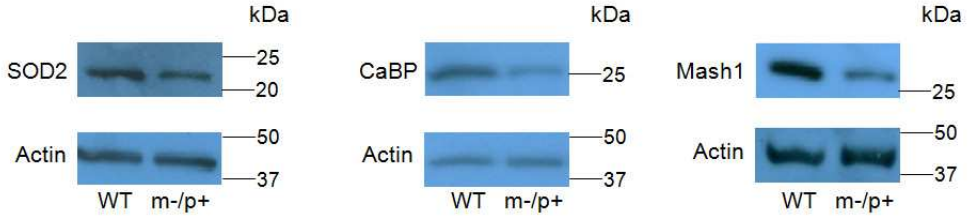

Fig. 5. Validation of down-regulation of SOD2, CaBP and Mash1 in the cerebellum of *Ube3a* knockout mice. SOD2, CaBP and Mash1 are down-regulated in AS mouse model. Antibody dilution factor used for Western blotting were- SOD2, 1:5000; CaBP, 1:5000; Mash1, 1:5000.

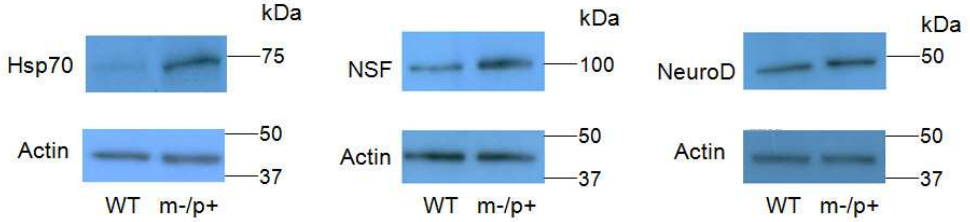

Fig. 6. Validation of proteins accumulated in the cerebellum of *Ube3a* knockout mice. Three proteins, including HSP70, NSF and NeuroD, are accumulated in AS mice. Antibody dilution factors used for Western blotting were- HSP70, 1:5000; NSF, 1:5000; and NeuroD, 1:5000.

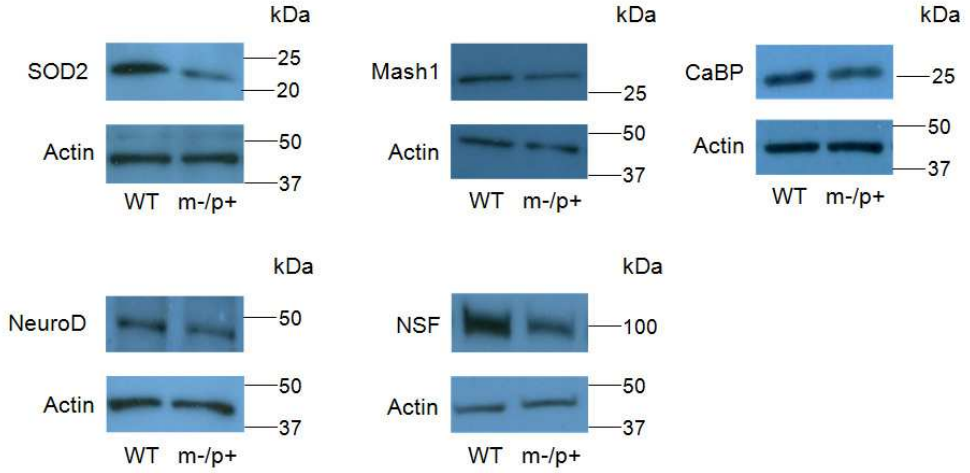

Fig. 7. Validation of down-regulated proteins in the hippocampus of *Ube3a* knockout mice. Five proteins, including SOD2, Mash1, CaBP, NeuroD and NSF, are down-regulated in AS mice. Antibody dilution factors used for Western blotting were-SOD2, 1:5000; Mash1, 1: NSF, 1:5000; NeuroD, 1:2500.

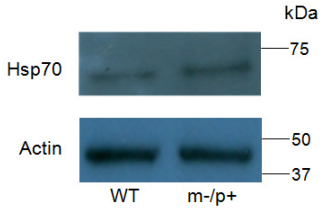

Fig. 8. Validation of Hsp70 accumulation in the hippocampus of *Ube3a* knockout mice. Hsp70 showed accumulation in AS mice among protein candidates detected by 2-D DIGE/MS. Antibody dilution factor used for Western blotting was- HSP70, 1:5000.

The major differences in the Western blot validation are the differential expressions of NeuroD and NSF in these two tissues. These two proteins were found to be up-regulated in the cerebellum but down-regulated in the hippocampus [Figure 9]. This suggests that the expression of these two proteins might be tissue specific. Western blot analysis for protein candidates VDR, LDH, MDH, GSTs-Mu1 and ATP5a1 has not been conducted due to the unavailability of antibodies when this study was conducted.

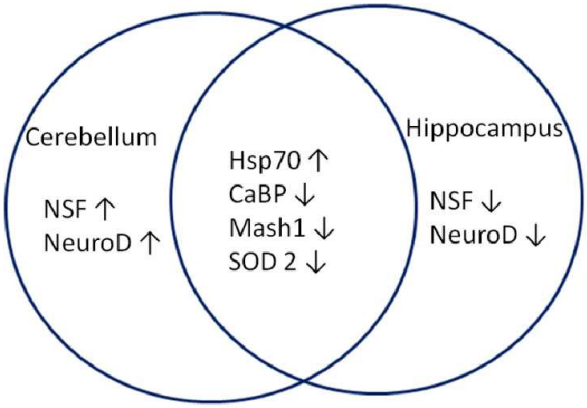

Fig. 9. A summary of the validation of 2-D DIGE/MS results by Western blot analysis. A total of 6 proteins from the cerebellum and hippocampus were tested by Western blot. Three of them, including CaBP, Nash1 and SOD2, were down-regulated and one (Hsp70) was up-regulated in both tissues, while both NSF and NeuroD showed tissue-specific expression patterns.

3.4 Transcriptional analysis of the differentially expressed proteins verified by Western blot analysis

Since variation of steady state protein level between wild type and mutant mice can be caused by enhancing transcriptional activity instead of enhancing protein half life, Real Time RT-PCR was conducted to quantify mRNA levels of proteins detected by 2-D DIGE. mRNA extracted from the cerebellum and hippocampus of wild type mice as well as *Ube3a* knockout mice were used in this study. Real Time RT-PCR was conducted at least three times for individual sets of mice. The Student's T-test was applied for this study.

Based on results of Real Time RT-PCR obtained from the cerebellum sample [Table 5], mRNA levels of *CaBP*, *NeuroD* and *VDR* were down-regulated by 57%, 33% and 55%, respectively. The mRNA levels of other proteins, including *Hsp70, SOD2, Mash1, Pax6, NSF, ATP5a1, LDH, MDH* and *Glutathione S-transferase Mu1,*were not affected in the AS mouse. Real Time RT-PCR revealed that mRNA levels of *CaBP, NeuroD, Pax6, VDR* and *LDH* were down-regulated in the hippocampus of *Ube3a* knockout mice by 80%, 85%, 82%, 72% and 45%, respectively, while the mRNA level of *Glutathione S-transferase Mu1* was up-regulated by 107% [Table 5]. In contrast, mRNA levels of *MDH*, *ATP5a1*, *NSF*, *Mash1*, *SOD2* and *Hsp70* were not affected in the hippocampus of *Ube3a* knockout mice.

Cerebellum		
Percentage changes (protein level)	Candidates	Percentage changes (mRNA level)
75% ↓	CaBP	57% ↓
75% ↓	Mash1	6% -
45% ↓	SOD2	13% -
120% ↑	HSP70	17% -
50% ↑	NeuroD	33% ↓
85% ↑	NSF	2% -
n/a	LDH	17% -
n/a	MDH	15% -
n/a	GSTs-Mu1	1% -
n/a	VDR	55% ↓
n/a	ATP5a1	12% -
n/a	Pax6	21% -
Hippocampus		
Percentage changes (protein level)	Candidates	Percentage changes (mRNA level)
40% ↓	CaBP	80% ↓
80% ↓	Mash1	12% -
80% ↓	SOD2	22% -
50% ↑	HSP70	25% -
45% ↓	NeuroD	85% ↓
50% ↓	NSF	6% -
n/a	LDH	45% ↓
n/a	MDH	14% -
n/a	GSTs-Mu1	107% ↑
n/a	VDR	72% ↓
n/a	ATP5a1	15% -
n/a	Pax6	82% ↓

Table 5. A summary of Western blot validation and Real Time RT-PCR analysis of candidates tested in the cerebellum and hippocampus of *Ube3a* knockout mice.

4. Discussion

When Ube3a was first identified as an E3 ligase, little was known about its targeting substrates besides p53 (1). However, as techniques improved over the years, additional substrates of Ube3a were identified [Table 6].

	Gene / Protein	Function	Reference
1	Src Family of Tyrosine Kinase Blk	Regulators of cytoskeletal organization, cell-cell contact, cell-matrix adhesion, DNA synthesis, cellular proliferation	(16)
2	Cystic fibrosis transmembrane regulator-associated ligand (CAL)	Facilitate of lysosomal degradation of other proteins, intracellular trafficking, autophagy of neuronal cells, vesicular trafficking pathways	(17)
3	Trihydrophobin 1 (TH1)	Assembly of functional human negative transcription elongation factor (NELF) complex	(18)
4	Epithelial call transforming sequence 2 oncogene (ECT2)	Cytokinesis, cytoskeletal remodelling in response to neurite guidance cues	(19)
5	Polyglutamine aggregation	Protein aggregation associated to cell death and neurodegenerative diseases	(20-22)

Table 6. Recently identified substrates of Ube3a

Among these proteins, Blk, from the tightly regulated Src family of non-receptor tyrosine kinase, is important in cytoskeletal organization, cell-cell contact, and cell-matrix adhesion; a few other proteins from the Src family are also interacting partners of Ube3a (16). Cystic fibrosis transmembrane regulator-associated ligands (CAL), which serve as membrane-associated scaffolds, are involved in the targeting of other plasma membrane proteins and autophagy in neuronal cells (17). Trihydrophobin 1 (TH1) is another interacting partner and target of Ube3a that was recently identified; it is an integral subunit of the human negative transcription elongation factor (NELF) complex, which is important in transcriptional pausing *in vitro* (18). ECT2 is involved in cytokinesis and cytoskeletal remodelling in response to all known neurite guidance cues (19). Its dysregulation may explain the general learning and behaviour defects in AS patients (4). Polyglutamine inclusion, which is translated from the expansion of a CAG trinucleotide repeat, causes several human neurodegenerative diseases, including spino-bulbar muscular atrophy (SBMA), Huntington's disease (HD) and the spinocerebellar ataxias (20-22).

In this study, we intended to examine the differential expression of proteins caused by the knockout of *Ube3a* in the AS model. By 2-D DIGE/MS, we identified proteins that are differentially expressed in the mutant mice, which may serve as the target substrates of Ube3a. The accumulation or reduction of these proteins may correlate with the phenotypes observed among AS patients.

From our 2-D DIGE/MS experiment and Western blot analysis using cerebellum [Figure 6] and hippocampus [Figure 8] tissue samples, up-regulation of Hsp70 was observed in *Ube3a* knockout mice. However, Real-Time RT-PCR analysis [Table 5] using RNA samples extracted from mice showed that Hsp70 mRNA levels were not significantly affected in the cerebellum and hippocampus when comparing *Ube3a* knockout and wild type mice. In conclusion, the differential expression of Hsp70 was observed only at the translational or protein level. It is conceivable that Hsp70 is the target of Ube3a, as Hsp70 is a multi-functional protein; its most prominent task is to serve as a chaperone in the ubiquitin proteasome system. Parkin and CHIP are two other E3-ligases that are known to interact with Hsp70 for protein quality control tasks (21). To perform its quality control task, Hsp70 serves as a chaperone that binds to misfolded proteins during translation or after stress-mediated protein damage. Studies have shown that Hsp70 interacts with co-chaperone CHIP, which functions as a RING domain E3-ligase, and together they serve as the protein quality control system that clears stress-damaged proteins from cells. Such proteins include tau in Alzheimer's disease and expanded polyglutamate protein in Huntington's disease (23,24). A recent study also demonstrated that E6AP reduces polyglutamate protein aggregation, which induces cell death. Results also showed that E6AP is over-expressed correlated with HSP70. The author suggested that HSP70 may play a modulatory role on the function of E6AP (20). Another study has also shown that Hsp70 is degraded through CHIP-dependent targeting to the ubiquitin-proteasome system (21). If E6AP does interact with Hsp70 to perform protein quality control, one of the possible scenarios might be that HSP70 is targeted by E6AP after the substrates have depleted. In the AS mouse model used in this study, *Ube3a* was knocked out; this might result in the accumulation of HSP70 after the target substrates have depleted. Ube3a may be acting in the positive feedback system, by promoting the degradation of HSP70 when HSP70 exceeds its threshold level in the body. The loss of Ube3a in knockout mice may prolong the half-life of Hsp70. As other studies have suggested, Hsp70 normally assists in multi-ubiquitin chain ubiquitination at lysine48 (K48), and such ubiquitination normally leads to the degradation of the protein (25). Even though there are other E3-ligases, all E3-ligases have their own specific targets. In addition, different post-translational modifications by Ube3a may have different effects on the protein and influence the range of functions that it performs (26). Lack of Ube3a may not only affect the half-life of Hsp70 but also affect the functions of Hsp70.

It is possible that Hsp70 might play a role in cell protection. In *Ube3a* knockout mice, there may be accumulation of other proteins that are specific substrates of Ube3a for degradation. Elevated levels of HSP70 may be triggered by accumulation of the substrate proteins or misfolded proteins. Studies have shown that elevated levels of HSP70 may assist in unfolding the misfolded proteins to prevent them from becoming toxins in the brain (27-31). This may also be the reason that protein aggregates commonly seen in other neurodegenerative diseases are absent in AS mouse models and AS patients. It is generally known that overexpression of HSP70 prior to neuronal insult improves cell survival in both stroke and epilepsy models. However according to recent studies, the neuroprotection effect from the expression of HSP70 in other neurodegenerative diseases was not observed in epileptogenic states, and over-expression of HSP70 in such cases only served as an indicator of neuronal stress in the acute phase of epilepsy (27). However, other studies have suggested that the death of neuronal cells is not caused by protein aggregation in the brain, but rather by the soluble intermediates. Accumulation of HSP70 may prevent the formation

of protein aggregation but allow soluble intermediates to cause toxic effects in AS patients. Both soluble intermediates and protein aggregates attribute to the clinical features of neurodegenerative diseases (32).

Expression of VDR is found to be reduced in *Ube3a* knockout mice at the protein level in this 2-D DIGE/MS study. We have also examined the mRNA level of VDR in the cerebellum and hippocampus of *Ube3a* knockout mice, and it is found to be down-regulated by 55% and 72%, respectively. Its ligand, vitamin-D_3, controls calcium homeostasis, bone formation, cell differentiation and apoptosis (33,34). The down-regulation of VDR may affect calcium homeostasis in mutant mice, as epilepsy is highly correlated with the disruption of calcium levels in cells and is one of the most well-known characteristics observed in Angelman syndrome patients. VDR is a transcriptional regulator that interacts with specific DNA sequences composed of hexanucleotide direct repeats and binds as either a homodimer or heterodimer with retinoid X receptors (RXRs); cell cycle inhibitors p21 and p27 are two known genes that VDR regulates (35,36). If VDR is down-regulated in *Ube3a* knockout mice, its upstream regulator BAG1L may also be affected. BAG1L, along with BAG1, BAG1M (Rap46), and BAG1S, are four protein isomers that the human BAG1 gene encodes. Recently, Hsp70 has been identified as a partner of BAGL1 in enhancing the trans-activation function of VDR in a concentration-dependent manner; this interaction has been speculated to improve tumor cell responses (37,38). Since BAG1L couples with Hsp70 to perform its functions, the accumulation of Hsp70 detected in the AS mouse model may be related to the down-regulation of VDR. VDR is a multifunctional protein that is known to regulate calcium homeostasis (33,34) and immunity (39). Therefore, the correlation between BAG1L, accumulation of Hsp70 and down-regulation VDR may be an interesting area to study in the *Ube3a* knockout model.

The homeostasis of Ca^{2+} in neurons can be achieved by the transportation of Ca^{2+} across the membrane, sequestration by cellular organelles, or with cytosolic buffering proteins such as pavalbumin and CaBP. Calcium ions, in turn, are actively involved in signal transduction, the development of regulatory proteins that modulate calcium ion transients, neurogenesis and many other functions. Lack of cytoplasmic CaBP severely impairs Ca^{2+} homeostasis and causes nerve cells to be selectively vulnerable to Ca^{2+} related injury (40,41). In the 2-D DIGE/MS study and Western blot analysis, CaBP was one of the proteins that was down-regulated in both cerebellum and hippocampus tissue of *Ube3a* knockout mice. It is known that the decline of CaBP in hippocampal dentate granule cells correlates with the kindling model for epilepsy; this may help to explain the frequent seizures observed among Angelman syndrome patients, as excess levels of intracellular Ca^{2+} may disrupt neuronal signal transduction (42).

Another study has shown that CaBP facilitates neuronal differentiation via up-regulation of genes such as *NeuroD*, *Pax6*, *VDR* and *Mash1* in a pathway involving CaMK (14). Mash1 or ASC1 is one of the basic helix-loop-helix (bHLH) transcription factors that heterodimerizes with the ubiquitous Class I bHLH E proteins to form complexes that are crucial in neurogenesis and neural differentiation during development (43). Adult neural progenitor cells continue to generate new neurons, astrocytes and oligodendrocytes in the brain throughout life, under normal turnover circumstances, or after ischemia in status epilepticus. Mash1 and Olig2 stimulate neurogenenesis and differentiation of progenitor cells in the telencephalon, generating the vast array of neurons and glia cells

found in the adult cerebral cortex and giving rise to the ganglionic eminence and olfactory epithelium (44,45). A study using Mash1 null mutant mice showed that Mash1 is required for the generation of an early population of oligodendrocyte precursors (OPCs), which is involved in the regulation of synaptic transmission and adult neurogenesis (46). Mice with a targeted deletion in Mash1 also fail to develop pulmonary neuroendocrine cells (PNECs), and they die in the neonatal period due to respiratory failure (47). NeuroD or Beta2 is another basic helix loop helix (bHLH) transcription factor expressed in neurons of the cortical plate, as well as neuroendocrine cells in the stomach, gut, pancreas and adult lung (48,49). It is involved in the differentiation of neurons and the development of the pancreas, inner ear and retina (48,50). Like other bHLH factors, it heterodimerizes with E proteins and controls the transcription of a variety of genes to induce neuron differentiation. When NeuroD is deleted in mice, the early differentiating pancreatic endocrine cells die, and total pancreatic insulin level is only about 5% of normal level. The mutant mice will eventually die within five days after birth due to hyperglycemia. In the hippocampus of NeuroD null mice, when the granule cells reach the dentate gyrus, both cell proliferation and differentiation are severely disturbed, leading to severe cellular depletion in the brain (49). The hippocampal mRNA and protein levels of CaBP have been demonstrated to express concurrently with the expression of these bHLH transcription factors (14). In the Real-Time RT-PCR study, fresh tissue from the AS mouse model was used instead of the progenitor cell cultures that were used in the previous study (14). This was to ensure that the *Ube3a* knockout environment was retained and was able to reflect the complex activity *in vivo*. In this case, *CaBP* mRNA levels were down-regulated by 57% in the cerebellum and 80% in the hippocampus; *NeuroD* mRNA levels were down-regulated concurrently by 33% and 85% in the cerebellum and hippocampus, respectively. However, *Mash1* mRNA levels remained unchanged in the two tissues. *NeuroD* encoding a bHLH protein is involved in neuronal cells development as well as differentiation; the down-regulation of *NeuroD* at mRNA levels may implicate the lack of differentiation in dendritic spines observed in the AS mouse model (51). Even though *Mash1* mRNA levels were unaffected, its protein levels were reduced in both the cerebellum and hippocampus of *Ube3a* knockout mice. On the other hand, *NeuroD* mRNA was down-regulated in the cerebellum and hippocampus, while NeuroD protein was accumulated in the cerebellum and down-regulated in the hippocampus. The deficiency of these two proteins in the hippocampus may not only affect the development and differentiation of cells but also affect neurogenesis after ischemic or neuronal damage.

Vitamin D_3 has been shown to induce the expression of CaBP (52,53), and vitamin D_3 receptor (VDR) and CaBP have been found to co-localize in many tissues, especially in the brain. Reduced *CaBP* and *VDR* mRNA levels in the hippocampus of neurodegenerative Alzheimer's disease have been reported (54). This coincides with our findings in the Real Time RT-PCR experiment that *CaBP* and *VDR* are down-regulated by 57% and 55%, respectively, in the cerebellum, and down-regulated by 80% and 72%, respectively, in the hippocampus of *Ube3a* knockout mice. Since both mRNA levels were affected and VDR protein levels were down-regulated in the 2D-DIGE analysis, this might correlate with the CaBP deficiency observed in the cerebellum and hippocampus. These findings demonstrate a specific association between VDR and CaBP.

Reactive oxygen species (ROS) are electronically activated species that have been shown to behave as signal transduction molecules that modulate protein function, such as facilitating oxidative posttranslational modification on protein chaperones (55,56). The intrinsic mitochondrial apoptotic pathway is the most common form of cell death in neurodegeneration; it controls the activation of caspase-9 by regulating the release of cytochrome c from the mitochondrial intermembrane space (IMS) (57). ROS are normal by-products of mitochondrial respiratory chain activity (58). ROS concentration is mediated by mitochondrial antioxidants such as manganese superoxide dismutase (SOD2) and glutathione peroxidase (59). Over production of ROS (oxidative stress) is a central feature of all neurodegenerative disorders (60). In addition to the generation of ROS, mitochondria are also involved in life-sustaining functions, including calcium homeostasis, mitochondrial fission and fusion, lipid concentration of the mitochondrial membranes and mitochondrial permeability transition (56,57,61). It is known that mice lacking SOD2 die several days after birth, amid massive oxidative stress (62). In our study, we observed that protein levels of SOD2 but not transcriptional levels were down-regulated in AS mice. Since SOD2 is vital for handling oxidative stress in mitochondria, down-regulation of SOD2 may cause a surge of oxidative damage in cells and eventually lead to cell death.

Lactate dehydrogenase (LDH), malate dehydrogenase (MDH) and Glutathione S-transferase Mu1 are found differentially expressed in the AS mice. These are proteins that are known to be involved in REDOX reactions. LDH catalyzes the interconversion of pyruvate and lactate with concomitant interconversion of NADH and NAD. Malate dehydrogenase (MDH) is an enzyme in the citric acid cycle that catalyzes the conversion of malate into oxaloacetate by using NAD^+. Pyruvate in the mitochondria is acted upon by pyruvate carboxylase to form oxaloacetate, a citric acid cycle intermediate (63,64). Glutathione S-transferase (GSTs) families consist of a total of eight sub-classes of isoenzymes, including alpha, kappa, mu, omega, pi, sigma, theta and zeta. These isoenzymes can be cytosolic, mitochondrial, or microsomal proteins depending on the site that they are acting on (65). Glutathione S-transferase Mu1 (GSTM1) is a human glutathione S-transferase. The mu class of enzymes functions mainly in the detoxification of electrophilic compounds, including carcinogens, therapeutic drugs, environmental toxins and products of oxidative stress, by conjugation with glutathione (GST) (66). Genetic variations of GSTM1 can change an individual's susceptibility to carcinogens and toxins, as well as affect the toxicity and efficacy of certain drugs. GSTM1 is essential for cell protection as reports show that GSTM1 null mice are predisposed to increased cancer risk due to increased susceptibility to environmental toxins and carcinogens (65,67,68). When SOD2, LDH, MDH and GSTs class mu1 are reduced in *Ube3a* knockout mice, mitochondrial defects are likely to occur, which may lead to neurodegeneration. Mitochondrial dysfunction and oxidative stress are implicated in the pathogenesis of neurodegenerative disease, which includes Alzheimer's disease, Parkinson's disease, Huntington's disease and Amyotrophic lateral sclerosis (ALS) (60,69). In the case of ALS, there are several proteins reported to have changes in expression that coincide with the *Ube3a* knockout mice used in this study; those proteins include ATP synthase, mitochondrial F1 complex α subunit; glutathione S-transferase class Mu1 and heat shock 70-kda protein (55). Intriguingly, in *parkin* knockout mice, a similar set of proteins is

found to be differentially expressed in the cortex and striatum, including ATP synthase α chain mitochondrial, lactate dehydrogenase, malate dehydrogenase, stress-70 protein, glutathione S-transferase P2 and N-ethylmaleimide-sensitive fusion protein (70). In the current study, protein levels of ATP synthase α chain mitochondrial, lactate dehydrogenase, malate dehydrogenase, stress-70 protein, glutathione S-transferase class Mu1, and N-ethylmaleimide-sensitive fusion protein are found to be differentially expressed in the AS mice. The mRNA levels of these proteins remained steady in mutant mice, except for LDH, which had a 55% down-regulation of mRNA levels, and glutathione S-transferase class Mu1, which had a 100% up-regulation of mRNA levels in the hippocampus. This showed that most of the proteins involved in REDOX are affected at the translational or protein level in the absence of functional Ube3a, thus suggesting that down-regulation of LDH, MDH and glutathione S-transferase class Mu1 at the protein level may play a crucial role in the pathogenesis of AS.

NSF is not affected at the transcriptional level in the cerebellum and hippocampus of *Ube3a* knockout mice, but it is specifically affected at the protein level. NSF is up-regulated in the cerebellum but down-regulated in the hippocampus of AS mice. NSF protein is thought to be involved in the docking and fusion of synaptic vesicles at the plasma membrane. It is known that transportation of neurotransmitters at the synapse, which involves synaptic vesicles fusing with the pre-synaptic membrane, relies on such processes to perform neuronal function. Studies have also shown that mutation of *NSF* in *Drosophila* can result in coma, presumably because neuronal functions have been blocked in the absence of NSF (71). AS patients exhibit symptoms such as tremor, ataxia and motor incoordination; a study has also shown motor dysfunction in *Ube3a* knockout mice (7). Since NSF is expressed abundantly in the hippocampus under normal circumstances (72), it is of interest to study the relationship between NSF deficiency in the hippocampus and movement incoordination in mutant mice. *NSF* has also been discovered as an epilepsy gene (73,74). Along with the discovery of CaBP deficiency in *Ube3a* knockout mice, these two proteins are crucial to the study of clinical features such as inducible seizures that are commonly found in AS patients.

In this study, we used the proteomic approach to study the effects of Ube3a deficiencies. Our results unveil that multiple proteins involved in redox reactions are affected and suggest that oxidative stress is associated with AS. Our results also indicated that proteins involved in neuronal cell differentiation, learning process, energy production, actin disassembly and likely neuronal signal transduction are affected in AS. Our findings provides clues for identification of therapeutic targets and for understanding of the detailed molecular mechanism of AS and other related neurological disorders.

5. Acknowledgements

The authors acknowledge financial support from the Academic Research Fund (M52080023) awarded to Ken-Shiung Chen and the grant from IAS Research Project (M58A40001).

6. References

[1] Jiang, Y., Lev-Lehman, E., Bressler, J., Tsai, T.F. and Beaudet, A.L. (1999) Genetics of Angelman syndrome. *Am J Hum Genet*, 65, 1-6.

[2] Witte, W., Nobel, C. and Hilpert, J. (2011) [Anesthesia and Angelman syndrome.]. *Anaesthesist*.

[3] Lalande, M. and Calciano, M.A. (2007) Molecular epigenetics of Angelman syndrome. *Cell Mol Life Sci*, 64, 947-960.

[4] Nicholls, R.D., Saitoh, S. and Horsthemke, B. (1998) Imprinting in Prader-Willi and Angelman syndromes. *Trends Genet*, 14, 194-200.

[5] Cattanach, B.M., Barr, J.A., Beechey, C.V., Martin, J., Noebels, J. and Jones, J. (1997) A candidate model for Angelman syndrome in the mouse. *Mamm Genome*, 8, 472-478.

[6] Culiat, C.T., Stubbs, L.J., Montgomery, C.S., Russell, L.B. and Rinchik, E.M. (1994) Phenotypic consequences of deletion of the gamma 3, alpha 5, or beta 3 subunit of the type A gamma-aminobutyric acid receptor in mice. *Proc Natl Acad Sci U S A*, 91, 2815-2818.

[7] Jiang, Y.H., Armstrong, D., Albrecht, U., Atkins, C.M., Noebels, J.L., Eichele, G., Sweatt, J.D. and Beaudet, A.L. (1998) Mutation of the Angelman ubiquitin ligase in mice causes increased cytoplasmic p53 and deficits of contextual learning and long-term potentiation. *Neuron*, 21, 799-811.

[8] Miura, K., Kishino, T., Li, E., Webber, H., Dikkes, P., Holmes, G.L. and Wagstaff, J. (2002) Neurobehavioral and electroencephalographic abnormalities in Ube3a maternal-deficient mice. *Neurobiol Dis*, 9, 149-159.

[9] Wu, M.Y., Chen, K.S., Bressler, J., Hou, A., Tsai, T.F. and Beaudet, A.L. (2006) Mouse imprinting defect mutations that model Angelman syndrome. *Genesis*, 44, 12-22.

[10] Jiang, Y.H., Pan, Y., Zhu, L., Landa, L., Yoo, J., Spencer, C., Lorenzo, I., Brilliant, M., Noebels, J. and Beaudet, A.L. (2010) Altered ultrasonic vocalization and impaired learning and memory in Angelman syndrome mouse model with a large maternal deletion from Ube3a to Gabrb3. *PLoS One*, 5, e12278.

[11] Johnstone, K.A., DuBose, A.J., Futtner, C.R., Elmore, M.D., Brannan, C.I. and Resnick, J.L. (2006) A human imprinting centre demonstrates conserved acquisition but diverged maintenance of imprinting in a mouse model for Angelman syndrome imprinting defects. *Hum Mol Genet*, 15, 393-404.

[12] Homanics, G.E., DeLorey, T.M., Firestone, L.L., Quinlan, J.J., Handforth, A., Harrison, N.L., Krasowski, M.D., Rick, C.E., Korpi, E.R., Makela, R. *et al.* (1997) Mice devoid of gamma-aminobutyrate type A receptor beta3 subunit have epilepsy, cleft palate, and hypersensitive behavior. *Proc Natl Acad Sci U S A*, 94, 4143-4148.

[13] Gabriel, J.M., Merchant, M., Ohta, T., Ji, Y., Caldwell, R.G., Ramsey, M.J., Tucker, J.D., Longnecker, R. and Nicholls, R.D. (1999) A transgene insertion creating a heritable chromosome deletion mouse model of Prader-Willi and angelman syndromes. *Proc Natl Acad Sci U S A*, 96, 9258-9263.

[14] Kim, J.H., Lee, J.A., Song, Y.M., Park, C.H., Hwang, S.J., Kim, Y.S., Kaang, B.K. and Son, H. (2006) Overexpression of calbindin-D28K in hippocampal progenitor cells increases neuronal differentiation and neurite outgrowth. *FASEB J*, 20, 109-111.

[15] Nawaz, Z., Lonard, D.M., Smith, C.L., Lev-Lehman, E., Tsai, S.Y., Tsai, M.J. and O'Malley, B.W. (1999) The Angelman syndrome-associated protein, E6-AP, is a coactivator for the nuclear hormone receptor superfamily. *Mol Cell Biol*, 19, 1182-1189.

[16] Oda, H., Kumar, S. and Howley, P.M. (1999) Regulation of the Src family tyrosine kinase Blk through E6AP-mediated ubiquitination. *Proc Natl Acad Sci U S A*, 96, 9557-9562.

[17] Jeong, K.W., Kim, H.Z., Kim, S., Kim, Y.S. and Choe, J. (2007) Human papillomavirus type 16 E6 protein interacts with cystic fibrosis transmembrane regulator-associated ligand and promotes E6-associated protein-mediated ubiquitination and proteasomal degradation. *Oncogene*, 26, 487-499.

[18] Yang, Y., Liu, W., Zou, W., Wang, H., Zong, H., Jiang, J., Wang, Y. and Gu, J. (2007) Ubiquitin-dependent proteolysis of trihydrophobin 1 (TH1) by the human papilloma virus E6-associated protein (E6-AP). *J Cell Biochem*, 101, 167-180.

[19] Reiter, L.T., Seagroves, T.N., Bowers, M. and Bier, E. (2006) Expression of the Rho-GEF Pbl/ECT2 is regulated by the UBE3A E3 ubiquitin ligase. *Hum Mol Genet*, 15, 2825-2835.

[20] Mishra, A., Dikshit, P., Purkayastha, S., Sharma, J., Nukina, N. and Jana, N.R. (2008) E6-AP promotes misfolded polyglutamine proteins for proteasomal degradation and suppresses polyglutamine protein aggregation and toxicity. *J Biol Chem*, 283, 7648-7656.

[21] Mishra, A., Godavarthi, S.K., Maheshwari, M., Goswami, A. and Jana, N.R. (2009) The ubiquitin ligase E6-AP is induced and recruited to aggresomes in response to proteasome inhibition and may be involved in the ubiquitination of Hsp70-bound misfolded proteins. *J Biol Chem*, 284, 10537-10545.

[22] Cummings, C.J., Reinstein, E., Sun, Y., Antalffy, B., Jiang, Y., Ciechanover, A., Orr, H.T., Beaudet, A.L. and Zoghbi, H.Y. (1999) Mutation of the E6-AP ubiquitin ligase reduces nuclear inclusion frequency while accelerating polyglutamine-induced pathology in SCA1 mice. *Neuron*, 24, 879-892.

[23] Rujano, M.A., Kampinga, H.H. and Salomons, F.A. (2007) Modulation of polyglutamine inclusion formation by the Hsp70 chaperone machine. *Exp Cell Res*, 313, 3568-3578.

[24] Rosser, M.F., Washburn, E., Muchowski, P.J., Patterson, C. and Cyr, D.M. (2007) Chaperone functions of the E3 ubiquitin ligase CHIP. *J Biol Chem*, 282, 22267-22277.

[25] Lim, K.L. and Lim, G.G. (2011) K63-linked ubiquitination and neurodegeneration. *Neurobiol Dis*, 43, 9-16.

[26] Yi, J.J. and Ehlers, M.D. (2007) Emerging roles for ubiquitin and protein degradation in neuronal function. *Pharmacol Rev*, 59, 14-39.

[27] Turturici, G., Sconzo, G. and Geraci, F. (2011) Hsp70 and its molecular role in nervous system diseases. *Biochem Res Int*, 2011, 618127.

[28] Magrane, J., Smith, R.C., Walsh, K. and Querfurth, H.W. (2004) Heat shock protein 70 participates in the neuroprotective response to intracellularly expressed beta-amyloid in neurons. *J Neurosci*, 24, 1700-1706.

[29] Cummings, C.J., Sun, Y., Opal, P., Antalffy, B., Mestril, R., Orr, H.T., Dillmann, W.H. and Zoghbi, H.Y. (2001) Over-expression of inducible HSP70 chaperone suppresses neuropathology and improves motor function in SCA1 mice. *Hum Mol Genet*, 10, 1511-1518.

[30] Jana, N.R., Tanaka, M., Wang, G. and Nukina, N. (2000) Polyglutamine length-dependent interaction of Hsp40 and Hsp70 family chaperones with truncated N-terminal huntingtin: their role in suppression of aggregation and cellular toxicity. *Hum Mol Genet*, 9, 2009-2018.

[31] Nagel, F., Falkenburger, B.H., Tonges, L., Kowsky, S., Poppelmeyer, C., Schulz, J.B., Bahr, M. and Dietz, G.P. (2008) Tat-Hsp70 protects dopaminergic neurons in midbrain cultures and in the substantia nigra in models of Parkinson's disease. *J Neurochem*, 105, 853-864.

[32] Yamamoto, A. and Simonsen, A. (2011) The elimination of accumulated and aggregated proteins: a role for aggrephagy in neurodegeneration. *Neurobiol Dis*, 43, 17-28.

[33] MacDonald, P.N., Haussler, C.A., Terpening, C.M., Galligan, M.A., Reeder, M.C., Whitfield, G.K. and Haussler, M.R. (1991) Baculovirus-mediated expression of the human vitamin D receptor. Functional characterization, vitamin D response element interactions, and evidence for a receptor auxiliary factor. *J Biol Chem*, 266, 18808-18813.

[34] Zinser, G., Packman, K. and Welsh, J. (2002) Vitamin D(3) receptor ablation alters mammary gland morphogenesis. *Development*, 129, 3067-3076.

[35] Glass, C.K. (1994) Differential recognition of target genes by nuclear receptor monomers, dimers, and heterodimers. *Endocr Rev*, 15, 391-407.

[36] Liu, M., Lee, M.H., Cohen, M., Bommakanti, M. and Freedman, L.P. (1996) Transcriptional activation of the Cdk inhibitor p21 by vitamin D3 leads to the induced differentiation of the myelomonocytic cell line U937. *Genes Dev*, 10, 142-153.

[37] Kudoh, M., Knee, D.A., Takayama, S. and Reed, J.C. (2002) Bag1 proteins regulate growth and survival of ZR-75-1 human breast cancer cells. *Cancer Res*, 62, 1904-1909.

[38] Guzey, M., Takayama, S. and Reed, J.C. (2000) BAG1L enhances trans-activation function of the vitamin D receptor. *J Biol Chem*, 275, 40749-40756.

[39] Welsh, J., Zinser, L.N., Mianecki-Morton, L., Martin, J., Waltz, S.E., James, H. and Zinser, G.M. (2011) Age-related changes in the epithelial and stromal compartments of the mammary gland in normocalcemic mice lacking the vitamin D3 receptor. *PLoS One*, 6, e16479.

[40] Dong, Z., Saikumar, P., Weinberg, J.M. and Venkatachalam, M.A. (2006) Calcium in cell injury and death. *Annu Rev Pathol*, 1, 405-434.

[41] Squier, T.C. and Bigelow, D.J. (2000) Protein oxidation and age-dependent alterations in calcium homeostasis. *Front Biosci*, 5, D504-526.

[42] Kohr, G., Lambert, C.E. and Mody, I. (1991) Calbindin-D28K (CaBP) levels and calcium currents in acutely dissociated epileptic neurons. *Exp Brain Res*, 85, 543-551.

[43] Henke, R.M., Meredith, D.M., Borromeo, M.D., Savage, T.K. and Johnson, J.E. (2009) Ascl1 and Neurog2 form novel complexes and regulate Delta-like3 (Dll3) expression in the neural tube. *Dev Biol*, 328, 529-540.

[44] Uchida, Y., Nakano, S., Gomi, F. and Takahashi, H. (2007) Differential regulation of basic helix-loop-helix factors Mash1 and Olig2 by beta-amyloid accelerates both differentiation and death of cultured neural stem/progenitor cells. *J Biol Chem*, 282, 19700-19709.

[45] Parras, C.M., Galli, R., Britz, O., Soares, S., Galichet, C., Battiste, J., Johnson, J.E., Nakafuku, M., Vescovi, A. and Guillemot, F. (2004) Mash1 specifies neurons and oligodendrocytes in the postnatal brain. *EMBO J*, 23, 4495-4505.

[46] Parras, C.M., Hunt, C., Sugimori, M., Nakafuku, M., Rowitch, D. and Guillemot, F. (2007) The proneural gene Mash1 specifies an early population of telencephalic oligodendrocytes. *J Neurosci*, 27, 4233-4242.

[47] Neptune, E.R., Podowski, M., Calvi, C., Cho, J.H., Garcia, J.G., Tuder, R., Linnoila, R.I., Tsai, M.J. and Dietz, H.C. (2008) Targeted disruption of NeuroD, a proneural basic helix-loop-helix factor, impairs distal lung formation and neuroendocrine morphology in the neonatal lung. *J Biol Chem*, 283, 21160-21169.

[48] Ross, S.E., Greenberg, M.E. and Stiles, C.D. (2003) Basic helix-loop-helix factors in cortical development. *Neuron*, 39, 13-25.

[49] Chae, J.H., Stein, G.H. and Lee, J.E. (2004) NeuroD: the predicted and the surprising. *Mol Cells*, 18, 271-288.

[50] Ochocinska, M.J. and Hitchcock, P.F. (2009) NeuroD regulates proliferation of photoreceptor progenitors in the retina of the zebrafish. *Mech Dev*, 126, 128-141.

[51] Ramocki, M.B. and Zoghbi, H.Y. (2008) Failure of neuronal homeostasis results in common neuropsychiatric phenotypes. *Nature*, 455, 912-918.

[52] Wasserman, R.H. and Taylor, A.N. (1966) Vitamin d3-induced calcium-binding protein in chick intestinal mucosa. *Science*, 152, 791-793.

[53] Thomasset, M., Parkes, C.O. and Cuisinier-Gleizes, P. (1982) Rat calcium-binding proteins: distribution, development, and vitamin D dependence. *Am J Physiol*, 243, E483-488.

[54] Sutherland, M.K., Somerville, M.J., Yoong, L.K., Bergeron, C., Haussler, M.R. and McLachlan, D.R. (1992) Reduction of vitamin D hormone receptor mRNA levels in Alzheimer as compared to Huntington hippocampus: correlation with calbindin-28k mRNA levels. *Brain Res Mol Brain Res*, 13, 239-250.

[55] Jain, M.R., Ge, W.W., Elkabes, S. and Li, H. (2008) Amyotrophic lateral sclerosis: Protein chaperone dysfunction revealed by proteomic studies of animal models. *Proteomics Clin Appl*, 2, 670-684.

[56] Squier, T.C. (2001) Oxidative stress and protein aggregation during biological aging. *Exp Gerontol*, 36, 1539-1550.

[57] Rego, A.C. and Oliveira, C.R. (2003) Mitochondrial dysfunction and reactive oxygen species in excitotoxicity and apoptosis: implications for the pathogenesis of neurodegenerative diseases. *Neurochem Res*, 28, 1563-1574.

[58] Sugawara, T., Noshita, N., Lewen, A., Gasche, Y., Ferrand-Drake, M., Fujimura, M., Morita-Fujimura, Y. and Chan, P.H. (2002) Overexpression of copper/zinc

superoxide dismutase in transgenic rats protects vulnerable neurons against ischemic damage by blocking the mitochondrial pathway of caspase activation. *J Neurosci*, 22, 209-217.

[59] Li, Q., Zhang, M., Chen, Y.J., Wang, Y.J., Huang, F. and Liu, J. (2011) Oxidative damage and HSP70 expression in masseter muscle induced by psychological stress in rats. *Physiol Behav*.

[60] Andersen, J.K. (2004) Oxidative stress in neurodegeneration: cause or consequence? *Nat Med*, 10 Suppl, S18-25.

[61] Scandalios, J.G. (1993) Oxygen Stress and Superoxide Dismutases. *Plant Physiol*, 101, 7-12.

[62] Zelko, I.N., Mariani, T.J. and Folz, R.J. (2002) Superoxide dismutase multigene family: a comparison of the CuZn-SOD (SOD1), Mn-SOD (SOD2), and EC-SOD (SOD3) gene structures, evolution, and expression. *Free Radic Biol Med*, 33, 337-349.

[63] Park, S.J., Cotter, P.A. and Gunsalus, R.P. (1995) Regulation of malate dehydrogenase (mdh) gene expression in Escherichia coli in response to oxygen, carbon, and heme availability. *J Bacteriol*, 177, 6652-6656.

[64] Courtright, J.B. and Henning, U. (1970) Malate dehydrogenase mutants in Escherichia coli K-12. *J Bacteriol*, 102, 722-728.

[65] Morari, E.C., Leite, J.L., Granja, F., da Assumpcao, L.V. and Ward, L.S. (2002) The null genotype of glutathione s-transferase M1 and T1 locus increases the risk for thyroid cancer. *Cancer Epidemiol Biomarkers Prev*, 11, 1485-1488.

[66] Berhane, K., Widersten, M., Engstrom, A., Kozarich, J.W. and Mannervik, B. (1994) Detoxication of base propenals and other alpha, beta-unsaturated aldehyde products of radical reactions and lipid peroxidation by human glutathione transferases. *Proc Natl Acad Sci U S A*, 91, 1480-1484.

[67] Tew, K.D. (1994) Glutathione-associated enzymes in anticancer drug resistance. *Cancer Res*, 54, 4313-4320.

[68] Parl, F.F. (2005) Glutathione S-transferase genotypes and cancer risk. *Cancer Lett*, 221, 123-129.

[69] Sorolla, M.A., Reverter-Branchat, G., Tamarit, J., Ferrer, I., Ros, J. and Cabiscol, E. (2008) Proteomic and oxidative stress analysis in human brain samples of Huntington disease. *Free Radic Biol Med*, 45, 667-678.

[70] Periquet, M., Corti, O., Jacquier, S. and Brice, A. (2005) Proteomic analysis of parkin knockout mice: alterations in energy metabolism, protein handling and synaptic function. *J Neurochem*, 95, 1259-1276.

[71] Pallanck, L., Ordway, R.W. and Ganetzky, B. (1995) A Drosophila NSF mutant. *Nature*, 376, 25.

[72] Puschel, A.W., O'Connor, V. and Betz, H. (1994) The N-ethylmaleimide-sensitive fusion protein (NSF) is preferentially expressed in the nervous system. *FEBS Lett*, 347, 55-58.

[73] Guan, Z., Lu, L., Zheng, Z., Liu, J., Yu, F., Lu, S., Xin, Y., Liu, X., Hong, J. and Zhang, W. (2001) A spontaneous recurrent seizure-related Rattus NSF gene identified by linker capture subtraction. *Brain Res Mol Brain Res*, 87, 117-123.

[74] Yu, F., Guan, Z., Zhuo, M., Sun, L., Zou, W., Zheng, Z. and Liu, X. (2002) Further identification of NSF* as an epilepsy related gene. *Brain research. Molecular brain research*, 99, 141-144.

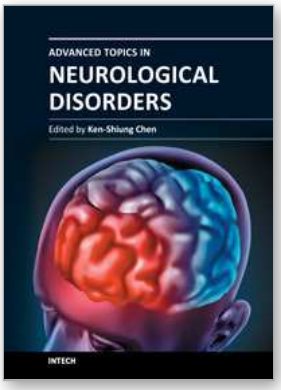

Advanced Topics in Neurological Disorders

Edited by Dr Ken-Shiung Chen

ISBN 978-953-51-0303-5
Hard cover, 242 pages
Publisher InTech
Published online 16, March, 2012
Published in print edition March, 2012

This book presents recent advances in the field of Neurological disorders research. It consists of 9 chapters encompassing a wide range of areas including bioengineering, stem cell transplantation, gene therapy, proteomic analysis, alternative treatment and neuropsychiatry analysis. It highlights the development of multiple discipline approaches in neurological researches. The book brings together leading researchers in neurological disorders and it presents an essential reference for researchers working in the neurological disorders, as well as for students and industrial users who are interested in current developments in neurological researches.

INTECH
open science | open minds

InTech Europe
University Campus STeP Ri
Slavka Krautzeka 83/A
51000 Rijeka, Croatia
Phone: +385 (51) 770 447
Fax: +385 (51) 686 166
www.intechopen.com

InTech China
Unit 405, Office Block, Hotel Equatorial Shanghai
No.65, Yan An Road (West), Shanghai, 200040, China
中国上海市延安西路65号上海国际贵都大饭店办公楼405单元
Phone: +86-21-62489820
Fax: +86-21-62489821